# Bifurcations in Haploid and Diploid Sequence Space Models

Ellen Baake[1] and Thomas Wiehe[2]

[1]Max-Planck-Institut für Entwicklungsbiologie, Spemannstr. 35, D-72076 Tübingen, Germany.
FAX: (+49) 7071 601 448
email: ellen@mpib-tuebingen.mpg.de
[2]Department of Integrative Biology, University of California, Berkeley, CA 94720, U.S.A.

**Abstract**

Deterministic models of mutation and selection in the space of (binary) nucleotide-type sequences have been investigated for haploid populations during the past 25 years, and, recently, for diploid populations as well. These models, in particular their 'error thresholds', have mainly been analyzed by numerical methods and perturbation techniques. We consider them here by means of bifurcation theory, which improves our understanding of both equilibrium and dynamical properties.

In a caricature obtained from the original model by neglecting back mutation to the favourable allele, the familiar error threshold of the haploid two-class model turns out to be a simple transcritical bifurcation, whereas its diploid counterpart exhibits an additional saddle node. This corresponds to a second error threshold. Three-class models with neutral spaces of unequal size introduce further features. Such are a global bifurcation in haploid populations, and simple examples of Hopf bifurcations (as predicted by Akin's theorem) in the diploid case.

Running title: Bifurcations in Sequence Space Models
Keywords: sequence space, selection, mutation, error threshold, Hopf bifurcations

# 1 Introduction

The study of the interplay between selection and mutation has a long history in evolutionary theory. In the twenties, Fisher (e.g. [10]) and Haldane (e.g. [14]) were the pioneers of mathematical models describing the joint effects of mutation and selection on allele frequencies in natural populations; for a review of subsequent developments, see [9]. In continuous time, a 'coupled' and a 'decoupled' version of the mutation-selection equation emerged, depending on whether or not mutation is assumed to be coupled to reproduction [6, 13].

With the discovery of the molecular structure of DNA and its replication mechanism, theoretical interest shifted towards models reflecting these features; among the first examples are the infinite site and the infinite allele models [20, 19]. Within the framework of reaction kinetics, Eigen [7] introduced a model describing the replication dynamics of biopolymers which incorporates the action of mutation and selection on the level of polynucleotide sequences. With a reinterpretation of parameters, this model may be considered as a *sequence space version* of the classical mutation-selection equation. Its haploid version has been investigated during the last two decades (for review, see [8]). Diploid versions have, however, been studied only recently [16, 4, 35]. As far as the action of *mutation* is concerned, the models do not distinguish between haploid and diploid organisms. The diploid *selection* mechanism, however, increases the order of the differential equations involved, thus introducing a wider range of possible behaviour.

A general treatment of sequence space dynamics, whether haploid or diploid, seems impossible due to the huge dimension of the space. To render the equations tractable, a high degree of symmetry for the selection parameters is usually assumed. Such a procedure, at the same time, justifies a deterministic approach. After all, even with moderate sequence lengths, the number of possible strings by far exceeds any realistic population size. An ODE approach, however, requires a very large number of individuals of every possible (geno-)type. Therefore, it cannot cope with sequence space unless additional symmetries are introduced to reduce the degrees of freedom.

Perhaps the simplest such scenario is the so-called single-peaked landscape, a two-class model with one favourable allele and mutants of reduced fitness (equal for all of them). In the haploid context, this toy model has long served to demonstrate the error threshold phenomenon, i.e. the virtual loss of the favourable allele due to accumulation of mutants when a critical mutation rate is surpassed [8]. The analysis is greatly simplified by the global convergence to the equilibrium [32]. Wiehe *et al.* [35] analyzed a straightforward diploid generalization and found that, other than in the haploid case, *bistability* may occur.

Error thresholds have been studied by means of perturbation analysis with mutation probability as perturbation parameter (see [28]). Being *local* in nature, these methods show how equilibria of the pure selection model are shifted due to (weak) mutation but fail to reveal certain global aspects.

Understanding the global behaviour requires the knowledge of *all* equilibria and the bifurcations they undergo for arbitrary mutation rates. Autocatalytic reaction networks with mutation were analyzed in this vein by Stadler *et al.* [29]. With mutation of the *coupled* type and without further simplifications, however, only special cases (like the Schlögl model) can be analyzed completely. In this paper, therefore, we use the simplest possible equation by starting from the *decoupled* version and neglecting back mutations from the mutants to the favourable allele. For certain fitness (or 'adaptive') landscapes, this yields ODE systems which are equivalent to models with few alleles that can be thoroughly discussed, in particular, all equilibria may be calculated. Analysis of their bifurcation structure will improve our understanding of error thresholds, on the one hand, and of dynamical properties, on the other. In particular, we shall characterize error thresholds and similar transition phenomena as bifurcations.

After recalling the mutation-selection equation, we revisit the haploid and diploid two-class models and show how the latter may give rise to *bistability* and to *two* error thresholds. As a generalization, a three-class model is introduced in Section 5. It exhibits various bifurcations, including a global bifurcation in the haploid version, and Hopf bifurcations in the diploid case (Section 6).

## 2 The model

Let us briefly recall the classical mutation-selection equation and its sequence space version. They have been dealt with in more detail in [17, 18] and [35].

If mutations are caused by external influences (like radiation) and if they may happen at any time during the life cycle of an organism, the appropriate ODE for the composition of an (infinite) diploid population with overlapping generations in Hardy-Weinberg proportions is the *decoupled* mutation-selection equation

$$\dot{x}_i \;=\; x_i\left((Wx)_i - (x, Wx)\right) + (Mx)_i \;, \qquad i = 1, \ldots, n \,, \tag{2.1}$$

as formulated by Crow and Kimura [6], and thoroughly investigated by Akin [1]. Here, $n$ is the number of alleles, and $x_i$ denotes the relative frequency of allele $A_i$ (with $\sum_i x_i = 1$). Recall that, in continuous time, Hardy-Weinberg proportions are only an approximation [12]; selection dynamics in terms of genotypes has been thoroughly investigated in [30, 31]. $W$ is the symmetric $n \times n$ matrix of Malthusian fitness parameters of (ordered) $A_iA_j$ genotypes, and $(Wx)_i := \sum_{j=1}^{n} w_{ij}x_j$ is the marginal fitness of allele $A_i$. With $(x, y)$ the usual scalar product of the vectors $x$ and $y$, $(x, Wx)$ is the average fitness of the population. $M$ is the mutation matrix with elements $m_{ij} := m_{i \leftarrow j}$ denoting the mutation rate from $A_j$ to $A_i$ for $i \neq j$, and $m_{ii} = -\sum_j m_{ji}$. In a previous paper [4], we introduced a sequence space version of this model. Considering as 'alleles' $S, T, \ldots$, all possible binary strings of length $\nu$, we have $n = 2^\nu$ and

$$m_{ST} = \begin{cases} \mu\,, & d(S,T) = 1 \\ -\nu\mu\,, & S = T \\ 0\,, & \text{otherwise} \end{cases} \tag{2.2}$$

where $\mu$ is the single digit mutation rate, and $d(S,T)$ is the Hamming distance [33] between $S$ and $T$.

The decoupled equation relies on the independence of mutation and selection events. If, instead, mutations are assumed to originate as replication errors on the occasion of reproduction events, one is led to the *coupled* mutation-selection equation as studied by Hadeler [13]. In [35], we analyzed in parallel sequence space versions of both models, finding very similar behaviour even at large mutation rates. Although sequence space models have mostly been studied in the coupled form, we will here rely on the mathematically simpler decoupled version.

## 3 The diploid two-class model

As a slight generalization of what has previously been called single-peaked landscape, consider a sequence of length $\nu$ with $\kappa$ 'selected' sites and $\nu - \kappa$ neutral ones. The latter might be due to synonymous codons, absence of functional constraints on the respective part of the molecule, or some other source of neutrality. We assume the selective properties of a sequence to depend only on whether it is 'correct' at all $\kappa$ prescribed positions (favourable class $B_1$) or not (mutant class $B_2$). That is, we only consider neutral spaces with a very simple structure (see [25] for a random graph approach to more general structures of neutral networks).

Denoting by $|B_i|$ the number of sequences in $B_i$, we obviously have $|B_1| = 2^{\nu-\kappa}$ and $|B_2| = 2^{\nu} - 2^{\nu-\kappa}$. As long as all mutation terms in (2.2) are respected, the size of the ODE system (2.1) remains unchanged. If we consider, however, a caricature of the original model by neglecting mutations from $B_2$ to $B_1$ (which is a good approximation if $|B_1| \ll |B_2|$, e.g., $\kappa > 3$), we may lump together as $y$ and $1-y$ the relative frequencies of all alleles in $B_1$ and $B_2$. This yields the equivalent of a classical two-allele model. Similar caricatures have proved useful before, e.g. in the analysis of stochastic models of error thresholds [24, 35]. Denoting by $W$ the corresponding $2 \times 2$ fitness matrix, the decoupled equation reads (note the factorization of the right-hand side)

$$\dot{y} = f(y) = y\, g(y)\,, \tag{3.1}$$

where

$$g(y) := \phi y(1-y) + r(1-y) - \kappa\mu \tag{3.2}$$

and

$$\phi := w_{11} + w_{22} - 2w_{12}\;, \quad r := w_{12} - w_{22}\,. \tag{3.3}$$

The signs of $r$, and $\phi + r = w_{11} - w_{12}$, may be used to classify the selection regime. Since our interest here is mainly in situations related to a single-peaked landscape, we will restrict ourselves to the sector $r \geq 0$, $\phi + r \geq 0$, i.e. $w_{11} \geq w_{12} = w_{21} \geq w_{22}$, but require one of the inequalities to be strict, i.e. exclude the neutral case. Then, for $\phi < 0$ ($\phi > 0$), $B_1$ is dominant (recessive). The case $\phi = 0$ is equivalent to $w_{12} = \frac{1}{2}(w_{11} + w_{22})$, i.e. intermediate fitness, and the diploid model reduces to the haploid one.

For $\mu = 0$ (i.e. the pure selection equation), $f(y) > 0$ for $y \in (0,1)$. Its zeros are

$$y^{(0)} = 0\,, \quad y^{(1)} = 1\,, \quad \text{and} \quad y^{(2)} = -\frac{r}{\phi}\,, \tag{3.4}$$

with

$$f'(y^{(0)}) = r\;, \quad f'(y^{(1)}) = -(\phi + r)\;, \quad f'(y^{(2)}) = -\frac{r(\phi + r)}{\phi}\;, \tag{3.5}$$

where $'$ denotes differentiation with respect to $y$. Let us first consider the generic case where $r > 0$, $\phi + r > 0$, and $\phi \neq 0$, i.e., $f(y)$ has three distinct zeros. Then, obviously, $y^{(0)}$ is unstable, and $y^{(1)}$ is stable. $y^{(2)}$ is the 'polymorphic' equilibrium and always outside $[0,1]$. For $\phi > 0$ ($\phi < 0$), $y^{(2)} < 0$ and stable ($y^{(2)} > 1$ and unstable).

To study the effect of mutation (which corresponds to subtracting the linear expression $\kappa\mu y$ from the cubic right-hand side of the selection equation), it is instructive to consider first arbitrary $\mu$ and *all* equilibria, although only those which are in $[0,1]$ for $\mu \geq 0$ are relevant. If they are presented in the $(\mu, y)$ plane, then trivial equilibria $y^{(0)}$ lie on the straight line $y = 0$ and $y^{(1)}$ and $y^{(2)}$ are located on a parabola (see Fig. 1). The straight line and the parabola intersect transversally at

$$\mu = \mu_1 := \frac{r}{\kappa}\,, \tag{3.6}$$

and the two nonlinear equilibria coalesce at the vertex $(\mu_2, \beta)$ of the parabola, where

$$\mu_2 := \frac{(\phi + r)^2}{4\kappa\phi}\;, \quad \text{and} \quad \beta := \frac{\phi - r}{2\phi}\,. \tag{3.7}$$

Since stabilities must alternate, this implies a transcritical bifurcation at $\mu = \mu_1$, and a saddle node at $\mu = \mu_2$ (see Fig. 1). For $\phi - r = 0$, one has $\mu_1 = \mu_2$, and the bifurcations coalesce into a pitchfork bifurcation. As to where and in which order these bifurcations occur, we distinguish the generic cases

1. $\phi - r > 0$: This is the most interesting case where both bifurcations take place in the relevant regime. To be more precise, $0 < \mu_1 < \mu_2$, and $0 < \beta < \frac{1}{2}$. This is the situation where the right-hand side of the selection equation changes from convex to concave in $(0, 1)$, thus admitting three points of intersection with a straight line.

2. $\phi - r < 0$, $\phi > 0$: Again, $0 < \mu_1 < \mu_2$, but now $\beta < 0$, that is, the saddle node is not relevant.

3. $\phi < 0$: Now, $\mu_2 < 0 < \mu_1$, and $\beta > 1$, that is, again, only the transcritical bifurcation is relevant.

For $\mu > 0$, the relevant sequence of events is thus the following. The trivial equilibrium $y^{(0)}$ is independent of $\mu$. For small $\mu$, the other equilibria are shifted, $y^{(1)}$ moving into the interior of $[0, 1]$ and $y^{(2)}$ towards (away from) $[0, 1]$ for $\phi > 0$ ($\phi < 0$). They inherit their stabilities from those of the selection equation. For larger $\mu$, we have for the cases as above:

1. At $\mu = \mu_1$, $y^{(2)}$ enters $[0, 1]$ via a transcritical bifurcation with $y^{(0)}$, after which $y^{(0)}$ is stable and $y^{(2)}$ is unstable. At $\mu = \mu_2$, $y^{(1)}$ and $y^{(2)}$ coalesce in a saddle node. That is, for $\mu_1 < \mu < \mu_2$, there is a bistable regime with $y^{(0)}$ and $y^{(1)}$ both stable, which may come somewhat unexpectedly in this monotonic fitness landscape.

2. and 3. In both cases, only the transcritical bifurcation is relevant. This time, it involves $y^{(1)}$ and $y^{(0)}$. After this, $y^{(0)}$ is stable. This is reminiscent of the usual error threshold.

For $\phi = 0$, the parabola degenerates into a straight line, and the saddle node does not occur (but the transcritical bifurcation remains). For $r = 0$ and $\phi + r = 0$, the right-hand side of the selection equation has a double zero, which implies $\mu_1 = 0$ and $\mu_2 = 0$, respectively.

Let us discuss the significance of these observations in terms of the biologically more familiar fitness scheme

$$w_{11} = 1 + 2s, \quad w_{12} = 1 + 2hs = w_{21}, \quad w_{22} = 1\,, \tag{3.8}$$

where $s > 0$ is the selective advantage and $h$ the dominance coefficient ($0 \leq h \leq 1$). This yields $r = 2sh$, $\phi = 2s(1-2h)$, and $\phi + r = 2s(1-h)$. The stability properties of the three equilibria are summarized in Fig. 1 for various values of $h$, where we have also included the overdominant case for comparison.

The haploid situation corresponds to $h = \frac{1}{2}$. Obviously, the usual error threshold of the haploid population on a single-peaked landscape emerges as a transcritical bifurcation in the caricature without back mutation. A bistable regime occurs for $0 \leq h < \frac{1}{3}$. Similar behaviour has been observed before by Bürger [5] for the two allele mutation-selection equation without back mutation, and by Stadler *et al.* for the two species reaction network with mutation [29]. We have previously constructed examples of multiple equilibria in the full sequence space version with several alleles and back mutation [35]. We may conclude that the error threshold is not unique; rather, there exist two error thresholds. Initial conditions decide which one is relevant. This hysteresis illustrates an important difference between haploid and diploid sequence space models. The global stability guaranteed in haploid versions as long as $\mu > 0$, cf. [23, 35], assures the identity between what we would like to call 'static' and 'dynamic' aspects of error thresholds. The static aspect refers to the question how much mutation a population can tolerate once it has found a fitness peak. This is the familiar question behind models of error thresholds (and of Muller's ratchet as well, see [34]). Dynamic aspects, on the other hand, result from the question of how much mutation a new favourable allele, initially present only in one or a few copies, can tolerate while still on its way to establish itself. In diploid situations, the answers need not be the same. In the bistable regime, the static error threshold is at $\mu_2$, whereas the dynamic one is at $\mu_1 < \mu_2$. In the extreme case of $h = 0$, the favourable allele is completely recessive and will never get established in the population if its initial frequency is low. This is related to the long substitution times of recessive alleles, as discussed in [3]. We conclude that, during 'evolution' (in its literal sense), a favourable allele may be more vulnerable to mutational loss than in a stationary state—independently of additional stochastic effects.

# 4 Simplex coordinates

In what follows, we will turn to situations with more than one favourable class $B_1, \ldots, B_{n-1}$, and the class $B_n$ comprising all other sequences. The ODE then lives on the $n-1$ dimensional unit simplex embedded in $\mathbb{R}^n$, which is, in barycentric coordinates,

$$S_{n-1} := \{x \mid x = \sum_{i=1}^{n} x_i \hat{e}_i \,,\; x_i \geq 0 \,,\; \sum_{i=1}^{n} x_i = 1\} \,, \tag{4.1}$$

where the $\hat{e}_i$ are the canonical unit vectors of $\mathbb{R}^n$. For our purposes, however, it turns out more convenient to choose

$$S_{n-1} = \{x | x = \hat{e}_n + \sum_{i=1}^{n-1} y_i (\hat{e}_i - \hat{e}_n) \,, y_i \geq 0,\; \sum_{i=1}^{n-1} y_i \leq 1\} \,, \tag{4.2}$$

where it is natural to distinguish the $\hat{e}_n$ vertex, which corresponds to the pure mutant population. This induces the following change of variables (already implicit in Eq. (3.1))

$$x = T\hat{y} \qquad \text{with} \qquad T = \begin{pmatrix} 1 & & & 0 \\ & 1 & & \\ & & \ddots & \\ -1 & \ldots & -1 & 1 \end{pmatrix} \tag{4.3}$$

and $\hat{y} = T^{-1}x$ where $T^{-1}$ is identical to $T$ with the minus signs omitted. Obviously, for $x \in S_{n-1}$, $\hat{y} = (x_1, \ldots, x_{n-1}, 1)^t$, and we take $y = (x_1, \ldots, x_{n-1})^t$ as the new vector of variables.

The average and marginal fitnesses transform accordingly:

$$(x, Wx)|_{S_{n-1}} = (\hat{y}, \widehat{W}\hat{y})|_{S_{n-1}} = (y, \Phi y) + 2(r, y) + w_{nn} \,, \tag{4.4}$$

where we have written $\widehat{W} := T^t W T = \widehat{W}^t$ as

$$\widehat{W} = \begin{pmatrix} \Phi & r \\ r^t & w_{nn} \end{pmatrix} . \tag{4.5}$$

Here, $\Phi$ is a symmetric $(n-1) \times (n-1)$ matrix and $r$ an $n-1$ vector. Explicitly,

$$r_i = w_{in} - w_{nn} \quad \text{and} \quad \phi_{ij} = w_{ij} - w_{in} - w_{jn} + w_{nn} . \tag{4.6}$$

For the marginal fitnesses, an elementary calculation yields

$$(Wx)_i|_{S_{n-1}} = (\Phi y)_i + (r, y) + r_i + w_{nn} , \quad i = 1, \ldots, n-1 . \tag{4.7}$$

Finally, the selection terms entering the ODE read

$$((Wx)_i - (x, Wx))\,|_{S_{n-1}} = r_i + (\Phi y)_i - (r, y) - (y, \Phi y) , \quad i = 1, \ldots, n-1 . \tag{4.8}$$

For an interpretation of $\Phi$ and $r$, consider the case of intermediate fitness, i.e., $w_{ij} = \frac{1}{2}(w_{ii} + w_{jj})$. In this case, $\Phi = 0$, and $r_i = \frac{1}{2}(w_{ii} - w_{nn})$, $i = 1, \ldots, n-1$. Obviously, the terms involving $\Phi$ vanish, and the $r_i$ may be interpreted as haploid selection parameters (relative to the fitness of the mutant class).

# 5 The haploid three-class model

It goes without saying that real fitness landscapes are not single-peaked; one would rather expect many possible proteins to serve a given purpose to varying extents, and with varying amounts of selective constraints associated with them. Inching towards reality, we now tackle a fitness landscape with two peaks. Let us consider the decoupled equation describing a haploid situation with two favourable classes $B_1$, $B_2$ which comprise all sequences that are 'correct' at $\kappa_1$, $\kappa_2$ selected (possibly overlapping) positions, and the mutant class $B_3$ comprising all other sequences. We only consider situations where $d(B_1, B_2) := \min\{d(S,T), S \in B_1, T \in B_2, i \neq j\} > 1$, which ensures that $B_1$ and $B_2$ are disjoint, and no direct mutation occurs between the two classes in the decoupled system. It also implies that $d(B_1, B_3) = d(B_2, B_3) = 1$, i.e., both favourable classes mutate into the non-favourable class directly. Using the notation of the previous Section, $\Phi = 0$, and $r_1, r_2 > 0$. The caricature without back mutation makes sense then as long as $|B_1| \ll |B_3|$, $|B_2| \ll |B_3|$, which may be assumed as long as $\kappa_1, \kappa_2 > 3$.

The decoupled system then reads

$$\dot{y}_i = f_i(y) = y_i g_i(y) = y_i \left( r_i - r_1 y_1 - r_2 y_2 - \kappa_i \mu \right) , \quad i = 1, 2. \tag{5.1}$$

It is actually equivalent to Lotka's competition model (see [18]),

$$\dot{y}_1 = y_1(a - b y_1 - c y_2) \tag{5.2}$$

$$\dot{y}_2 = y_2(d - e y_1 - f y_2) . \tag{5.3}$$

Ours is the special case $a = r_1 - \kappa_1 \mu$, $d = r_2 - \kappa_2 \mu$, $b = e = r_1$, $c = f = r_2$. In this case, the nontrivial null clines, the straight lines $g_1(y) = 0$ and $g_2(y) = 0$, are always parallel and coalesce when $a = d$. That is, mutual exclusion holds except in this nongeneric case. In genetical terms, this means that there are, in general, no polymorphisms in the sense that, at equilibrium, at least one of the three types is absent.

The equilibria of the ODE (5.1) are (disregarding the restriction to $S_2$ for the moment)

(A) $y_1 = y_2 = 0$ (pure $B_3$ population);

(B) $y_1 = 0, g_2(y) = 0$ ($B_2 B_3$ population);

(C) $g_1(y) = 0, y_2 = 0$ ($B_1 B_3$ population);

(D) $g_1(y) = g_2(y) = 0$ (polymorphic population): This is the nongeneric situation where the nontrivial null clines coalesce, and one has a *line* of equilibria, which passes through (B) and (C).

The stabilities are seen immediately on drawing the null clines in the $y_1, y_2$ phase plane, as in Fig. 2. We assume $r_1 \neq r_2$ to avoid nongeneric cases, and take $r_1 > r_2$ without loss of generality. Then, for $\mu = 0$, (C) is stable, (B) a saddle and the origin (A) is unstable. When $\mu$ is allowed to vary (and the other parameters are fixed), the nontrivial null clines pass the origin at $\mu = \mu_1 := \frac{r_1}{\kappa_1}$ and $\mu = \mu_2 := \frac{r_2}{\kappa_2}$, respectively, giving rise to transcritical bifurcations of (C) resp. (B) with the origin, (A). If $\kappa_1 \neq \kappa_2$, the nontrivial null clines coalesce when $\mu$ passes through $\mu_0 := \frac{r_1 - r_2}{\kappa_1 - \kappa_2}$. In this case, (B) and (C) exchange their stabilities *across* the line (D). This is a kind of global bifurcation in the sense that, at $\mu = \mu_0$, the phase portrait is not structurally stable.

Where and in which order these bifurcations happen depends on the relative magnitudes of the selection and mutation pressures. We have to distinguish the following cases:

1. $\kappa_1 < \kappa_2$: The distance of the null clines increases with $\mu$, and $\mu_0 < 0 < \mu_2 < \mu_1$. This implies that only the transcritical bifurcations are relevant, and (C) is the stable equilibrium until it hits the origin. This is not too astonishing: $B_1$ is not only the fitter but also the larger of the two favourable classes, due to its larger number of neutral positions. It is thus advantageous in any respect and over the entire range of mutation rates and (C) should be expected to lose stability last.

2. $\kappa_1 = \kappa_2 = \kappa$: Now, the nontrivial null clines remain at a constant distance from each other for all $\mu$, $\mu_0$ does not exist, and $0 < \mu_2 < \mu_1$. Again, (C) is the stable equilibrium until it hits the origin. This is because $B_1$ and $B_2$ have the same number of selected positions but $B_1$ is fitter.

3. $\kappa_1 > \kappa_2$: We will exclude the nongeneric case $\mu_1 = \mu_2$ and distinguish

   (a) $\mu_1 < \mu_2$: This implies $0 < \mu_0 < \mu_1 < \mu_2$ . The nontrivial null clines move towards each other with increasing $\mu$, penetrating each other at $\mu = \mu_0$. The bifurcation sequence is shown in Fig. 2. For $0 < \mu < \mu_0$, the stable equilibrium is (C) but 'jumps' to (B) across the line (D) when $\mu$ passes through $\mu_0$. Increasing $\mu$ further leads to loss of (C) from $S_2$ at $\mu = \mu_1$, and of (B) at $\mu = \mu_2$, after which the origin is the only equilibrium in $S_2$, and is stable.

   In this case, the less fit sequence has fewer selected positions and is thus less vulnerable to mutation. It is inferior to the fittest string as long as mutation rates are small but outcompetes it at higher mutation. The remarkable feature of this transition is the discontinuity in the position of the stable equilibrium, in contrast to the (continuous) transcritical bifurcation of the haploid error threshold.

A situation with two favourable classes, a tall narrow peak in sequence space competing with a less high but broader one has been studied by Schuster and Swetina [27] with the help of numerical simulations and analytical approximations. They observe the transition between the two kinds of quasispecies to be remarkably sharp, in contrast to the usual continuous error threshold. The underlying nature of these two thresholds is clarified by the above bifurcation analysis.

(b) $\mu_1 > \mu_2$: Now, $0 < \mu_2 < \mu_1 < \mu_0$, and the null clines coalesce *after* leaving the simplex. Although the fitter class has the larger number of selected positions to maintain, its selective advantage is large enough to compensate for this. It will always expel the less fit class from the population.

# 6 The diploid three-class model

We now turn to caricatures of diploid three-class models. We will first consider the case

## 6.1 Neutral spaces of equal size

In this case, we have $\kappa_1 = \kappa_2 = \kappa$, i.e. the ODE reads

$$\dot{y}_i = f_i(y) = y_i \, g_i(y), \quad i = 1, 2, \tag{6.1}$$

where (cf. (4.8))

$$g_i(y) = r_i + (\Phi y)_i - (r, y) - (y, \Phi y) - \kappa\mu \tag{6.2}$$

(recall that $\Phi$ is a symmetric $2 \times 2$ matrix). Note that, due to $\kappa_1 = \kappa_2 = \kappa$, the mutation rates of the system in barycentric coordinates have the form $m_{ij} = m_i$ for $i \neq j$, with $m_1 = m_2 = 0, m_3 = \kappa\mu$. It has been shown by Hofbauer [17] that, in this special case, the differential equation is a gradient system with respect to the Shahshahani metric, as long as it is confined to $\mathring{S}_{n-1}$, the interior of $S_{n-1}$. This guarantees that all orbits converge to the set of equilibria, and the eigenvalues of the linearization at these equilibria are real. In particular, periodic orbits are excluded.

Instead of the fitness matrix $W$, we regard $\Phi$ and $r$ from Section 4 as the primitive parameters of our model. More precisely, we consider matrices $\Phi$ with the following properties:

$$\begin{aligned} \Phi^t &= \Phi && (6.3)\\ \det(\Phi) &\neq 0 && (6.4)\\ \phi_{11}\phi_{22} &\neq 0 && (6.5)\\ \phi_{11} + \phi_{22} - 2\phi_{12} &\neq 0 && (6.6)\\ \phi_{12} \neq \phi_{11} \quad &, \quad \phi_{12} \neq \phi_{22}\,. && (6.7) \end{aligned}$$

The symmetry of $\Phi$ results from the symmetry of $W$, and assumption (6.4) serves to exclude nongeneric cases (it excludes $\phi_{12}$ to be the geometric mean of $\phi_{11}$ and $\phi_{22}$). We further assume non-intermediate fitness for all pairs of alleles, i.e., $w_{ij} \neq \frac{1}{2}(w_{ii} + w_{jj})$, $i, j = 1, 2, 3$, which yields eqs. (6.5) and (6.6). The meaning of eq. (6.7) becomes clear on inspection of the equilibria of (6.1). Due to the factorization of the right-hand side, equilibria occur on the $y_1$- and $y_2$-axis (like in the haploid three-class model), or when $g_1(y) = g_2(y) = 0$ (which occurs generically now in contrast to the haploid case). The latter condition implies

$$g_1(y) - g_2(y) = (\Phi y)_1 - (\Phi y)_2 + (r_1 - r_2) = 0\,, \tag{6.8}$$

that is, the intersections of the nontrivial null clines are on a straight line which is independent of $\mu$. Thus, all equilibria lie on (at least) one of the three straight lines defined by $y_1 = 0$, $y_2 = 0$, and eq. (6.8), and bifurcations are expected where these intersect. Condition (6.7) just implies that the line (6.8) intersects both axes transversally. That it is also transversal to the line through $(1,0)^t$ and $(0,1)^t$ (which we will call the $B_1B_2$-line in the following) follows already from (6.4).

Note that the $y_1$- and $y_2$-axes are invariant under the flow (6.1). Obviously, the flow on every axis corresponds to a two-class situation as dealt with in detail in Section 3. It has a similar bifurcation structure with transcritical and saddle-node bifurcations, which may give rise to several stable equilibria and several error thresholds. We will, however, not go into the details here, but instead concentrate on the less obvious equilibria defined by eq. (6.8).

As motivated by the treatment of the selection equation [21], we write the equilibrium condition in the following form

$$\Phi y + r = ((y, \Phi y + r) + \kappa\mu)\, e\ , \tag{6.9}$$

where $e := (1,1)^t$. We now define the scalar auxiliary function

$$\alpha(y,\mu) := (y, \Phi y + r) + \kappa\mu\,, \tag{6.10}$$

with which (6.9) becomes

$$\Phi y + r = \alpha(y,\mu) e\,. \tag{6.11}$$

This may be rearranged as ($\Phi$ is nonsingular!)

$$y = \alpha(y,\mu)\Phi^{-1}e - \Phi^{-1}r\,. \tag{6.12}$$

Inserting eqn. (6.11) and (6.12) into the right-hand side of (6.10), we obtain a quadratic equation in $\alpha(y,\mu)$, with coefficients independent of $y$,

$$\alpha^2(y,\mu)(e,\Phi^{-1}e) - \alpha(y,\mu)\left(1 + (e,\Phi^{-1}r)\right) + \kappa\mu = 0\,. \tag{6.13}$$

Its solutions (which we will not need explicitly) depend on $\mu$ only, $\alpha(y,\mu) \equiv \alpha(\mu)$. From them, $y$ may be obtained explicitly via (6.12).

Let us first comment on the equilibria in the case $\mu = 0$. Then, eq. (6.13) has the solutions

$$\alpha^{(1)}(0) = \frac{1 + (e,\Phi^{-1}r)}{(e,\Phi^{-1}e)}\ , \quad \text{and} \quad \alpha^{(2)}(0) = 0\ . \tag{6.14}$$

The equilibrium corresponding to $\alpha^{(2)}$ (denoted by $y^{(2)}$) does, in general, not lie on any of the straight lines that contain the edges of $S_2$. We will thus call it the 'polymorphic' equilibrium in the following, and abbreviate it by

$$\eta := -\Phi^{-1}r\,. \tag{6.15}$$

For $y = \eta$, all marginal fitnesses equal the average fitness (cf. eq. (4.8)). If $\eta \in \mathring{S}_2$, it is usually called the 'interior' equilibrium [18]. Our usage of the term 'polymorphic' is meant to include equilibria outside $S_2$.

For $y^{(1)} = \eta + \alpha^{(1)}(0)\Phi^{-1}e$, on the other hand, one has $(e, y^{(1)}) = 1$, that is, this equilibrium is on the $B_1B_2$ line (though not necessarily on the edge of $S_2$).

We will return to these pure selection equilibria later. Let us first calculate the linearization for our equilibria with arbitrary $\mu$ (i.e. arbitrary $\alpha$). Let $y$ be any of $y^{(1)}$, $y^{(2)}$. Since $g_1(y) = g_2(y) = 0$, the elements of the Jacobian read $J_{ij} = y_i(\phi_{ij} - 2(\Phi y)_j + r_j)$. Using the equilibrium condition in the form (6.11), one obtains

$$J = Y(U - \alpha(\mu)\, ee^t)\,, \tag{6.16}$$

where $U := \Phi - e(\Phi y)^t$, and $Y := \mathrm{diag}(y_1, y_2)$. For its determinant, we calculate

$$\begin{aligned} \det(J) &= y_1y_2\,(\det(U) - \alpha(\mu)(\bar{e}, \Phi\bar{e})) \\ &= y_1y_2 \det(\Phi)(1 - (e, y) - \alpha(\mu)(e, \Phi^{-1}e))\,, \end{aligned} \tag{6.17}$$

where $\bar{e} := (1, -1)^t$. The trace reads

$$\mathrm{tr}(J) = y_1(1 - y_1)\phi_{11} + y_2(1 - y_2)\phi_{22} - 2y_1y_2\phi_{12} - \alpha(\mu)(y_1 + y_2)\,. \tag{6.18}$$

From the gradient property of the flow, no complex eigenvalues can occur as long as the equilibria are confined to $\mathring{S}_2$. To proceed with the analysis, we now change our point of view and let the coordinates of the *equilibrium*, $y_1$ and $y_2$, vary, whereas $\Phi$ and the auxiliary parameter $\alpha$ are assumed fixed. Then, $r$ is determined by (6.11) (i.e., $r = \alpha e - \Phi y$), and $\mu$ is calculated by inserting the equilibrium condition (6.11) into the definition of $\alpha$ (6.10), which yields $\kappa\mu = \alpha(1 - y_1 - y_2)$. The advantage of this inverse point of view is that it renders the problem linear.

For later use, we first show

**Lemma 1** *Let $\Phi$ fulfil assumptions* (6.3)–(6.7)*, and $\alpha$ be fixed. Then, the curve $\mathcal{C}_1 := \{\mathrm{tr}(J) = 0\}$ (from eq.* (6.18)*) in the $y_1$-$y_2$-plane has only transversal intersections with the straight lines that contains the edges of $S_2$, namely*

1. *with the line $\{y_2 = 0\}$ provided $\alpha \neq \phi_{11}$,*
2. *with the line $\{y_1 = 0\}$ provided $\alpha \neq \phi_{22}$,*
3. *with the line $\{y_1 + y_2 = 1\}$ provided $\alpha \neq \frac{1}{4}(\phi_{11} + \phi_{22} - 2\phi_{12})$.*

*Proof.* $\mathcal{C}_1$ is a conic section. It intersects the straight lines at

$$\begin{aligned} \mathcal{C}_1 \cap \{y_2 = 0\} &= \{s^{(0)}, s^{(1)}\}\,, \qquad s^{(0)} := (0,0)^t,\; s^{(1)} := (1 - \frac{\alpha}{\phi_{11}}, 0)^t \\ \mathcal{C}_1 \cap \{y_1 = 0\} &= \{s^{(0)}, s^{(2)}\}\,, \qquad s^{(2)} := (0, 1 - \frac{\alpha}{\phi_{22}})^t \\ \mathcal{C}_1 \cap \{y_1 + y_2 = 1\} &= \{s^{(3)}, s^{(4)}\}\,, \qquad s^{(3,4)} := \frac{1}{2}\left(e \pm \bar{e}\sqrt{1 - \frac{4\alpha}{\phi_{11} + \phi_{22} - 2\phi_{12}}}\right)\,. \end{aligned}$$

Under the assumptions made, the two points of each intersection are distinct. □

Let us now return to the equilibria without mutation. For the polymorphic equilibrium $y = \eta$ as characterized by $\alpha = 0$, we show

**Lemma 2** *If $\eta \in \overset{\circ}{S}_2$, then $J$ has the same stability as $\Phi$.*

*Proof.* For $\alpha = 0$, $J$ may be written as

$$J = C\Phi \ , \quad \text{where} \quad C := Y(I - ey^t) = \begin{pmatrix} y_1(1-y_1) & -y_1y_2 \\ -y_1y_2 & y_2(1-y_2) \end{pmatrix}$$

is obviously symmetric and positive definite since $y_1, y_2$, and $1 - y_1 - y_2$ are all positive ($y = \eta \in \overset{\circ}{S}_2$). Thus, $C^{1/2}$ exists and is real symmetric, and $J$ is similar to $\tilde{J} := C^{1/2}\Phi C^{1/2}$, which is obviously congruent to $\Phi$. So the statement follows from Sylvester's theorem [22]. □

Let us now turn to the case where the polymorphic equilibrium (still without mutation) is in the complement of $\overset{\circ}{S}_2$ (here and in what follows, 'complement' is meant w.r.t. the $y_1$-$y_2$–plane). Then the flow need no longer behave gradient-like. To analyze this case, we adopt the inverse point of view introduced above. Then, $\alpha = 0$, $\Phi$ is fixed, and the $y_1$-$y_2$–plane is considered as the parameter plane. Then, $r = -\Phi y$ from the equilibrium condition (6.11). We look for Hopf bifurcations, which occur if there is a curve along which $\mathrm{tr}(J) = 0$, $\mathrm{grad}(\mathrm{tr}(J)) \neq 0$, and $\det(J) > 0$ (see [11]). Applying Lemma 1, we find

**Lemma 3** *If $\Phi$ fulfils assumptions* (6.3)–(6.7)*, the following statements are equivalent:*
*(i)* $\det(\Phi) < 0$*.*
*(ii) There is a curve $\mathcal{C}_3$ in the complement of $S_2$ (w.r.t. the $y_1$-$y_2$–plane) along which* $\mathrm{tr}(J) = 0$*,* $\mathrm{grad}(\mathrm{tr}(J)) \neq 0$*, and* $\det(J) > 0$*.*

*Proof.* Let us consider the curves $\mathcal{C}_1 = \{\mathrm{tr}(J) = 0\}$ (from Lemma 1) and $\mathcal{C}_2 := \{\det(J) = 0\}$ in the $y_1$-$y_2$–plane. The latter is the union of the straight lines $\{y_1 = 0\}$, $\{y_2 = 0\}$, and $\{y_1 + y_2 = 1\}$. They divide the plane into regions of equal sign of $\det(J)$, with opposite sign in regions sharing an edge. It is helpful to colour the regions accordingly (shaded where $\det(J) > 0$, white otherwise) as is shown in Fig. 3.

The curve $\mathcal{C}_1$ is a conic section. From the proof of Lemma 1, we know three distinct real points of $\mathcal{C}_1$, with the straight lines that join them *not* belonging to $\mathcal{C}_1$; thus, $\mathcal{C}_1$ is neither a straight line nor a pair of straight lines. Since $\Phi$ is nonsingular, $\mathcal{C}_1$ cannot be a parabola either. Thus, $\mathcal{C}_1$ can only be a nondegenerate ellipse or hyperbola. The gradient of $\mathrm{tr}(J)$ w.r.t. $y$ does not vanish (except at the centre of the conic section). Thus, we may take as $\mathcal{C}_3$ the part of $\mathcal{C}_1$ that passes through a shaded region.

From Lemma 1 and its proof, $\mathcal{C}_1$ intersects transversally two of the three straight lines of $\mathcal{C}_2$ at every vertex of $S_2$. Since these are the only points $\mathcal{C}_1$ and $\mathcal{C}_2$ have in common, (branches of) $\mathcal{C}_1$ can never pass from a shaded to a white region or vice versa. Whether they reside in shaded or white regions can be decided by looking at (the signs of) $\mathrm{tr}(J)$ on the edges of $S_2$. We have

$$\begin{aligned} \mathrm{tr}(J)|_{y_2=0} &= y_1(1-y_1)\phi_{11} \\ \mathrm{tr}(J)|_{y_1=0} &= y_2(1-y_2)\phi_{22} \\ \mathrm{tr}(J)|_{y_1+y_2=1} &= y_1y_2(\phi_{11}+\phi_{22}-2\phi_{12}) \ . \end{aligned}$$

Consider now the vertices of $S_2$. If $\mathrm{tr}(J)$ has different signs on the two edges of $S_2$ that meet at a vertex, the branch of $\mathcal{C}_1$ containing that vertex passes into $\overset{\circ}{S}_2$ through the vertex; it thus resides in regions of the same colour as $\mathring{S}_2$. The opposite is true of a branch of $\mathcal{C}_1$ that contains a vertex which is formed by two edges with same sign of $\mathrm{tr}(J)$. Then, the branch remains outside $\mathring{S}_2$, in regions with shading different from that of $\mathring{S}_2$. Explicitly, we have the following cases (see Fig. 3):

1. $\det(\Phi) > 0$: $\det(J)$ is positive in $\mathring{S}_2$, and $\mathcal{C}_1$ is an ellipse. $\phi_{11}$, $\phi_{22}$, and $\phi_{11}+\phi_{22}-2\phi_{12}$ all have the same sign (since $\phi_{11}\phi_{22} > 0$, and $(\phi_{11}+\phi_{22})(\phi_{11}+\phi_{22}-2\phi_{12}) \geq 2\phi_{11}\phi_{22}+\frac{1}{2}(\phi_{11}+\phi_{22})^2 - 2\phi_{12}(\phi_{11}+\phi_{22}) \geq \frac{1}{2}(\phi_{11}-2\phi_{12}+\phi_{22})^2 > 0$ , where we have used $\det(\Phi) > 0$, $a^2+b^2 \geq \frac{(a+b)^2}{2}$, and assumption (6.6)). Hence, $\mathcal{C}_1$ only passes through regions with $\det(J) \leq 0$.

2. $\det(\Phi) < 0$: Now $\det(J)$ is negative in $\mathring{S}_2$, and the colouring of the plane is induced correspondingly. $\mathcal{C}_1$ is a hyperbola. There are two cases:

   (a) $\phi_{11}$, $\phi_{22}$, and $\phi_{11}+\phi_{22}-2\phi_{12}$ all have the same sign. One branch of $\mathcal{C}_1$ contains all vertices of $S_2$. It passes through shaded regions.

   (b) $\phi_{11}$, $\phi_{22}$, and $\phi_{11}+\phi_{22}-2\phi_{12}$ do not all have the same sign. Now one of the branches of $\mathcal{C}_1$ passes through $\mathring{S}_2$ (which is white), and through white regions outside. The other branch passes through the shaded region outside $S_2$.

   So, in both cases (a) and (b), a curve $\mathcal{C}_3$ with the properties required can be found in the complement of $S_2$.

□

From the biological point of view, we need not bother about equilibria outside the simplex. However, the result just formulated will turn out very useful for the understanding of the Hopf bifurcations that occur *inside* $S_2$ as soon as $\kappa_1 \neq \kappa_2$.

We are finally ready to examine the case with mutation, i.e. $\alpha \neq 0$. $\Phi$ and $\alpha$ are fixed, $y_1$ and $y_2$ are allowed to vary, and $r$ and $\mu$ are determined in the manner described above.

We may then state

**Lemma 4** *Let $\Phi$ have properties (6.3)–(6.7), $\alpha \neq 0$, and not both $\alpha = \phi_{11}$ and $\alpha = \phi_{22}$. Then there is a curve $\mathcal{C}_3$ in the complement of $\mathring{S}_2$ along which $\mathrm{tr}(J) = 0$, $\mathrm{grad}(\mathrm{tr}(J)) \neq 0$, and $\det(J) > 0$.*

*Proof.* From eq. (6.17), $\det(J)$ changes sign across the $y_1$- and $y_2$–axes (as in the above case $\alpha = 0$), and across the straight line $\{y_1 + y_2 + \alpha(e, \Phi^{-1}e) - 1 = 0\}$ (see Fig. 4 for the colouring of the plane according to the sign of $\det(J)$). The latter intersects the axes at $d^{(1)} := (1 - \alpha(e, \Phi^{-1}e), 0)^t$ and $d^{(2)} := (0, 1 - \alpha(e, \Phi^{-1}e))^t$. For $\alpha \neq \phi_{11}$, $\mathcal{C}_1$ intersects the $y_1$-axis transversally at $s^{(1)} = (1 - \frac{\alpha}{\phi_{11}}, 0)^t$ (see proof of Lemma 1). Then, $s^{(1)} \neq d^{(1)}$, since $\alpha \neq 0$ and, from (6.7), $\det(\Phi) \neq (\phi_{11} + \phi_{22} - 2\phi_{12})\phi_{11}$. Thus, there is an open disc around $s^{(1)}$ that is cut into two half discs of opposite colour by $\mathcal{C}_2$. From continuity and transversality, $\mathcal{C}_1$ must pass through both. We thus have a curve $\mathcal{C}_3$ as asserted. An analoguous argument holds if $\alpha \neq \phi_{22}$. With the same reasoning as in the proof of Lemma 3, we thus have Hopf bifurcations in all cases that obey the assumptions. From the gradient properties of the flow, these cannot take place within $\mathring{S}_2$. (Note that the latter argument holds for arbitrary $\alpha$, since the mutation vector field is a Shahshahani gradient for positive as well as negative $\mu$.) So the bifurcations are confined to the complement of $\mathring{S}_2$. $\square$

Let us finally turn to the diploid three-class model with

## 6.2 Neutral spaces of unequal sizes

Then, our system reads

$$\dot{y}_i = f_i(y) = y_i \, g_i(y) \,, \tag{6.19}$$

$$g_i(y) = r_i + (\Phi y)_i - (r, y) - (y, \Phi y) - \kappa_i \mu \,, \quad i = 1, 2 \,, \tag{6.20}$$

with $\kappa_1 \neq \kappa_2$. The mutation vector field is no longer a Shahshahani gradient. From Akin's theorem [1] we know that there exist selection vector fields s.t. the combined mutation-selection vector field undergoes a Hopf bifurcation. The proof may be used to construct examples, as has been done for the related case of the recombination-selection equation [2], and for sequence space mutation [4]. The construction procedure is, however, quite complicated (actually, the use of symbolic manipulation packages is indispensable), which obscures an understanding of the resulting examples. Hofbauer [17] provides a simple example where cyclic mutation is destabilized by a selection vector field, giving rise to stable limit cycles. Cyclic mutation is, however, hard to interpret in molecular terms. Let us now have a look at what our caricature has to offer. For this purpose, equilibria on the axes need not be considered, so we again concentrate on the equilibria defined by $g_1(y) = g_2(y) = 0$. Geometrically, this describes the intersection of a conic section with a straight line, whose distance from the origin varies with $\mu$ (in contrast to the previous case where the straight line (6.8) was independent of $\mu$). In order to determine its solutions in a manner similar to (6.9), we first write $k := (\kappa_1, \kappa_2)^t$ as

$$k = c_1 e + c_2 \bar{e} \,, \tag{6.21}$$

where $c_1 := \frac{1}{2}(\kappa_1 + \kappa_2)$, $c_2 := \frac{1}{2}(\kappa_1 - \kappa_2)$ (obviously, the relevant regime is $c_1 > 0$, $-c_1 < c_2 < c_1$). We further abbreviate $\tilde{c}_1 := c_1 \mu$, $\tilde{c}_2 := c_2 \mu$. The equilibrium condition then reads

$$\Phi y + r = \alpha(y, \mu) e + \tilde{c}_2 \bar{e} \,, \tag{6.22}$$

where now

$$\alpha(y, \mu) := (y, \Phi y + r) + \tilde{c}_1 \,. \tag{6.23}$$

Applying the same procedure as in (6.11)–(6.12), one obtains $\alpha(y, \mu) \equiv \alpha(\mu)$ as the solution of

$$(\alpha(\mu))^2 (e, \Phi^{-1} e) - \alpha(\mu) \left(1 + (e, \Phi^{-1} r) - 2\tilde{c}_2 (\bar{e}, \Phi^{-1} e)\right) + \tilde{c}_2^2 (\bar{e}, \Phi^{-1} \bar{e}) - \tilde{c}_2 (\bar{e}, \Phi^{-1} r) + \tilde{c}_1 = 0 \,. \tag{6.24}$$

We will not need the solution explicitly. Exploiting the equilibrium condition as in Section 6.1, we obtain for the Jacobian

$$J = Y(\Phi - e(\Phi y)^t - \alpha \, e e^t - \tilde{c}_2 \, e \bar{e}^t) \,, \tag{6.25}$$

and hence

$$\det(J) = y_1 y_2 \det(\Phi) \left(1 - y_1 - y_2 - \alpha(\mu)(e, \Phi^{-1} e) - \tilde{c}_2 (\bar{e}, \Phi^{-1} e)\right) \,, \tag{6.26}$$

$$\mathrm{tr}(J) = y_1(1 - y_1)\phi_{11} + y_2(1 - y_2)\phi_{22} - 2 y_1 y_2 \phi_{12} - \alpha(\mu)(y_1 + y_2) + \tilde{c}_2 (y_2 - y_1) \,. \tag{6.27}$$

We will again consider the curves of zeros of $\mathrm{tr}(J)$ and $\det(J)$, $\mathcal{C}_1$ and $\mathcal{C}_2$, in the $y_1$-$y_2$–plane. This time, the parameters are $\Phi$, $\alpha$, and $\tilde{c}_2$, and $r$ and $\tilde{c}_1$ are obtained along the same lines as in Section 6.1. We can finally state

**Theorem** *For every $\Phi$ with properties* (6.3)–(6.7), *we can find values for $\alpha$ and $\tilde{c}_2$ for which there is a curve $\mathcal{C}_3$ in $\mathring{S}_2$ s.t.* $\mathrm{tr}(J) = 0$, $\mathrm{grad}(\mathrm{tr}(J)) \neq 0$, *and* $\det(J) > 0$.

*Proof.* From eq. (6.26), $\det(J)$ changes sign across the $y_1$- and $y_2$–axes (as in the above case $\alpha = 0$), and across the straight line $\{y_1 + y_2 + \alpha(e, \Phi^{-1}e) - \tilde{c}_2(\bar{e}, \Phi^{-1}e) - 1 = 0\}$ (see Fig. 5). The latter intersects the axes at

$$\begin{aligned} d^{(1)} &:= (1 - (\alpha + \tilde{c}_2)(e_1, \Phi^{-1}e) - (\alpha - \tilde{c}_2)(e_2, \Phi^{-1}e), 0)^t , \\ d^{(2)} &:= (0, 1 - (\alpha + \tilde{c}_2)(e_1, \Phi^{-1}e) - (\alpha - \tilde{c}_2)(e_2, \Phi^{-1}e))^t . \end{aligned}$$

From eq. (6.27), $\mathcal{C}_1$ intersects the $y_1$- and $y_2$–axes at the origin, and at

$$s^{(1)} := (1 - \frac{\alpha + \tilde{c}_2}{\phi_{11}}, 0)^t \quad \text{and} \quad s^{(2)} := (0, 1 - \frac{\alpha - \tilde{c}_2}{\phi_{22}})^t ,$$

respectively. With the same reasoning as in Lemma 1, the intersections are transversal as long as $\alpha + \tilde{c}_2 \neq \phi_{11}$ and $\alpha - \tilde{c}_2 \neq \phi_{22}$, respectively. Now, we choose $\alpha + \tilde{c}_2$ s.t. $0 < s_1^{(1)} < 1$. Then, by adjusting $\alpha - \tilde{c}_2$, $d_1^{(1)}$ can be made to take any prescribed value (since $(e_2, \Phi^{-1}e) \neq 0$ from assumption (6.7)). If $\det(\Phi) > 0$, we choose $d_1^{(1)} > s_1^{(1)}$; otherwise, we choose $d_1^{(1)} < s_1^{(1)}$. Then, there is an open disc around $s^{(1)}$, cut into two half discs of opposite colour by $\mathcal{C}_2$, s.t. the open half disc in $\mathring{S}_2$ is entirely in the shaded region. With the same arguments as in the proof of Lemma 4, we can conclude that there is a curve $\mathcal{C}_3$ that meets our assertions, and is this time in $\mathring{S}_2$. □

We have thus found Hopf bifurcations which are relevant in that they take place in $\mathring{S}_2$; it must finally be determined whether they also occur at positive mutation rates. To this end, we note that, from the definition of $\alpha$ (6.23)),

$$\alpha + \tilde{c}_2 = (y, \Phi y + r) + \kappa_1 \mu \quad \text{and} \quad \alpha - \tilde{c}_2 = (y, \Phi y + r) + \kappa_2 \mu . \tag{6.28}$$

Inserting the equilibrium condition (6.22) into eq.(6.28), one obtains

$$\begin{aligned} \tilde{c}_1 + \tilde{c}_2 &= (\alpha + \tilde{c}_2)(1 - y_1) - (\alpha - \tilde{c}_2) y_2 & (6.29) \\ \tilde{c}_1 - \tilde{c}_2 &= (\alpha - \tilde{c}_2)(1 - y_2) - (\alpha + \tilde{c}_2) y_1 . & (6.30) \end{aligned}$$

*If* the bifurcation is nondegenerate (see below), we can find rational $y_1$ and $y_2$ for which limit cycles exist. If, in addition, $\alpha$ and $\tilde{c}_2$ are chosen rational (as is, of course, possible in the above procedure), $\tilde{c}_1 + \tilde{c}_2$ and $\tilde{c}_1 - \tilde{c}_2$ are rational numbers. Then, we can find integer $\kappa_1, \kappa_2$ and a (rational) $\mu$ s.t. $\kappa_1 \mu = \tilde{c}_1 + \tilde{c}_2$ and $\kappa_2 \mu = \tilde{c}_1 - \tilde{c}_2$. In order to identify situations with $\kappa_1 \mu, \kappa_2 \mu > 0$, consider the case $\det(\Phi) > 0$ and $\phi_{11} > \phi_{12} > \phi_{22} > 0$. Then, $0 < \alpha + \tilde{c}_2 < \phi_{11}$ yields $0 < s_1^{(1)} < 1$. As to $d_1^{(1)}$, we note that $(e_1, \Phi^{-1}e) = \frac{1}{\det(\Phi)}(\phi_{22} - \phi_{12}) < 0$, and $(e_2, \Phi^{-1}e) = \frac{1}{\det(\Phi)}(\phi_{11} - \phi_{12}) > 0$. Inspection of (6.29) and (6.30) then shows that, provided $s_1^{(1)}$ is close enough to 0, and the open disc around $s^{(1)}$

is small enough, we can find $\alpha - \tilde{c}_2 > 0$ s.t. both $\tilde{c}_1 + \tilde{c}_2$ and $\tilde{c}_1 - \tilde{c}_2$ are positive in that disc.

The theorem just proved is, in a sense, complementary to Akin's as applied to the caricature of the diploid three-class model. The latter says that there exists a family of selection vector fields characterized by fitness matrices $W(\lambda)$ s.t. the combined vector field undergoes a Hopf bifurcation at $\lambda = 0$. The family $W(\lambda)$ is constructed from equilibria and mutation rates which may be chosen arbitrarily. Here, we may choose arbitrary $\Phi$, the non–intermediate fitness parameters, and find equilibria and mutation rates s.t. Hopf bifurcations take place. What neither theorem guarantees is the existence of *stable* limit cycles; the bifurcation might as well be subcritical or degenerate. Symbolic manipulation packages may be used to perform normal form calculations for single examples. We refrain from doing so, however, since it does not add much insight. Instead, we present a supercritical (numerical) example in Fig. 6. This is the remarkable situation of complicated behaviour in quite an inconspicuous fitness landscape (monotonic on $S_2$, due to $w_{11} > w_{22} > w_{33}$, and $w_{ii} > w_{ij} > w_{jj}$ for $i < j$). For small mutation rates, there is a saddle-node connection, which then breaks up in favour of a stable limit cycle.

# 7 Discussion

We have tackled caricatures of decoupled sequence space mutation-selection models with two and three fitness classes. They lead to a characterization of error thresholds and similar transition phenomena as bifurcations. In the simplest example, the well-known error threshold of the haploid single-peaked landscape emerges as a transcritical bifurcation. The diploid single-peaked landscape exhibits both a transcritical and a saddle node bifurcation, providing for bistability. As a consequence, one finds two error thresholds in such models, associated with a 'static' and 'dynamic' aspect of evolution, respectively. Establishing a favourable mutant may be much more sensitive to mutation than is maintenance of genetic information. In the extreme case, it may be impossible, even in a single-peaked fitness landscape. Let us remark that the situation of bistability due to the presence of both a saddle node and a transcritical bifurcation also occurs in a simple harvesting model in theoretical ecology with logistic growth of the vegetation and a constant number of herbivores [26]; see also [36]. The caricature of the haploid three-class model exhibits a global bifurcation which explains the behaviour of the 'quasi-degenerate quasispecies' observed before numerically and with the help of approximations [27].

The diploid three-class model with neutral spaces of equal size provides a natural example of a mutation vector field which is a Shahshahani gradient. In the interior of the simplex, the flow is therefore gradient-like. However, Hopf bifurcations lurk outside. This is biologically irrelevant but of great help in understanding the bifurcations guaranteed as soon as the neutral spaces have unequal size: They move into the interior.

Stable limit cycles have been constructed for the *recombination* selection equation, numerically in discrete time by Hastings [15], and analytically in continuous time by Akin [2]. All cycles found so far (including the examples in this paper) have very long periods. As discussed in [15, 2], this behaviour is relevant in at least two ways. First, it provides another possible cause of cycling in populations. Second, and more importantly, it implies a note of caution. Changes in gene (or phenotypic) frequencies observed in natural populations or selection experiments and attributed to environmental changes or directional selection might actually result from cyclic behaviour, with a period far too long to observe in real populations.

The fitness matrices observed to produce limit cycles in the recombination-selection equation all seem rather special, however, in that they exhibit a high degree of marginal underdominance and a particular type of (strong) epistasis [15, 2]. Our example for the mutation-selection equation suggests that genetic cycling may be a more general phenomenon that also occurs in quite natural situations with a monotonic fitness landscape.

# 8 Acknowledgements

We are grateful to J. von Below, A. Gierer, G. Jetschke, and K. Sigmund for helpful discussions, to M. Baake, S. Rotter and W. Stephan for critically reading the manuscript, and to K.P. Hadeler for valuable suggestions improving the presentation of the results. F. Haubensak lent us his assistance in fighting against computer bugs.

# References

[1] Akin, E.: The Geometry of Population Genetics (Lect. Notes Biomath. 31). New York: Springer 1979

[2] Akin, E.: Cycling in simple genetic systems. J. Math. Biol. **13**, 305–324 (1982)

[3] Baake, E.: Diploid sequence space, dominance, and evolution. Proc. 4th Int. Conf. on Math. Population Dynamics, in press (1996)

[4] Baake, E.: Diploid models on sequence space. J. Biol. Syst. **3**, 343–349 (1995)

[5] Bürger, R.: On the evolution of dominance modifiers I. A nonlinear analysis. J. Theor. Biol. **101**, 585–598 (1983)

[6] Crow, J. F., Kimura, M.: An Introduction to Population Genetics Theory. New York: Harper & Row 1970

[7] Eigen, M.: Selforganization of matter and the evolution of biological macromolecules. Naturwiss. **58**, 465–523 (1971)

[8] Eigen, M., McCaskill, J., Schuster, P.: The molecular quasi–species. Adv. Chem. Phys. **75**, 149–263 (1989)

[9] Ewens, W. J.: Mathematical Population Genetics. Berlin: Springer 1979

[10] Fisher, R. A.: On the dominance ratio. Proc. Roy. Soc. Edinb. **42**, 321–341 (1922)

[11] Guckenheimer, J., Holmes, P.: Nonlinear oscillations, dynamical systems, and bifurcations of vector fields. New York: Springer 1983

[12] Hadeler, K. P.: On the equilibrium states in certain selection models. J. Math. Biol. **1**, 51–56 (1974)

[13] Hadeler, K. P.: Stable polymorphisms in a selection model with mutation. SIAM J. Appl. Math. **41**, 1–7 (1981)

[14] Haldane, J. B. S.: A mathematical theory of natural and artificial selection. Part V: Selection and mutation. Proc. Camb. Phil. Soc. **23**, 838–844 (1928)

[15] Hastings, A.: Stable cycling in discrete-time genetic models. Proc. Natl. Acad. Sci. USA **78**, 7224–7225 (1981)

[16] Higgs, P. G.: Error thresholds and stationary mutant distributions in multi–locus diploid genetics models. Genet. Res., Camb. **63**, 63–78 (1994)

[17] Hofbauer, J.: The selection mutation equation. J. Math. Biol. **23**, 41–53 (1985)

[18] Hofbauer, J., Sigmund, K.: The Theory of Evolution and Dynamical Systems. Cambridge: CUP 1988

[19] Kimura, M.: The number of heterozygous nucleotide sites maintained in a finite population due to steady flux of mutations. Genetics **61**, 893–903 (1969)

[20] Kimura, M., Crow, J. F.: The number of alleles that can be maintained in a finite population. Genetics **49**, 725–738 (1964)

[21] Kingman, J. F. C.: A mathematical problem in population genetics. Proc. Camb. Phil. Soc. **57**, 574–582 (1961)

[22] Lang, S.: Linear Algebra. Reading (Mass.): Addison-Wesley 1970

[23] Moran, P. A. P.: Global stability of genetic systems governed by mutation and selection. Math. Proc. Camb. Phil. Soc. **80**, 331–336 (1976)

[24] Nowak, M., Schuster, P.: Error thresholds of replication in finite populations. Mutation frequencies and the onset of Muller's ratchet. J. Theor. Biol. **137**, 375–395 (1989)

[25] Reidys, C., Stadler, P., Schuster, P.: Generic properties of combinatory maps: neutral networks of RNA secondary structures. Bull. Math. Biol., in press (1996)

[26] Richter, O.: Simulation des Verhaltens ökologischer Systeme: Mathematische Methoden und Modelle. Weinheim: Verlag Chemie 1985

[27] Schuster, P., Swetina, J.: Stationary mutant distributions and evolutionary optimization. Bull. Math. Biol. **50**, 635–660 (1988)

[28] Stadler, P., Schuster, P.: Mutation in autocatalytic reaction networks. An analysis based on perturbation theory. J. Math. Biol. **30**, 597–632 (1992)

[29] Stadler, P. F., Schnabl, W., Forst, C. V., Schuster, P.: Dynamics of small autocatalytic reaction networks. II: Replication, mutation and catalysis. Bull. Math. Biol. **57**, 21–61 (1995)

[30] Szucs, J. M.: Equilibria and dynamics of selection at a diallelic autosomal locus in the Nagylaki–Crow continuous model of a monoecious population. J. Math. Biol. **31**, 317–349 (1993)

[31] Szucs, J. M.: Equilibria and dynamics of selection at a diallelic autosomal locus in the Nagylaki–Crow continuous model of a monoecious population with random mating II. The case of constant fertilities. J. Math. Biol. **31**, 601–609 (1993)

[32] Thompson, C. J. and McBride, J. L.: On Eigen's theory of the self-organization of matter and the evolution of biological macromolecules. Math. Biosci. **21**, 127–142 (1974)

[33] van Lint, J. H.: Introduction to Coding Theory. New York: Springer 1982

[34] Wagner, G. P., Krall, P.: What is the difference between models of error thresholds and Muller's ratchet. J. Math. Biol. **32**, 33–44 (1993)

[35] Wiehe, T., Baake, E., Schuster, P.: Error propagation in reproduction of diploid organisms. A case study on single peaked landscapes. J. Theor. Biol. **177**, 1–15 (1995)

[36] Yodzis, P.: Introduction to theoretical ecology. New York: Harper & Row 1989

## Figure Captions

Fig. 1: Equilibria of the diploid two-class model, eq. (3.1), with fitness parameters as in eq. (3.8) for various values of $h$. Horizontal axes: $\mu$; vertical axes: $y$.
From top left to bottom right: $h = 0,\ 1/5,\ 1/3,\ 1/2,\ 1,\ 3/2$. Other parameters: $s = 1/20,\ \kappa = 30$. Bold lines: stable equilibria; thin lines: unstable equilibria. Note that there are two (biologically relevant) stable equilibria for $h = 1/5$.

Fig. 2: Null clines and equilibria of the haploid three-class model, eq. (5.1), for various values of $\mu$. Other parameters: $r_1 = 1, r_2 = 9/10, \kappa_1 = 50, \kappa_2 = 30$.
Horizontal axis: $y_1$; vertical axis: $y_2$, $0 \leq y_1, y_2 \leq 1$. Bullets: stable equilibria; open circles: unstable equilibria; crossed circles: saddle points. Straight lines: null clines of the differential equation; arrows indicate the direction of the flow.

Fig. 3: Illustration of Proof of Lemma 3 (Hopf bifurcations at the polymorphic equilibrium, $\alpha = 0$).
Conic sections: zeros of $\mathrm{tr}(J)$ as in eq. (6.18). Bold straight lines: zeros of $\det(J)$ as in eq. (6.17). Horizontal axis: $y_1$; vertical axis: $y_2$. Shaded regions: $\det(J) > 0$; white regions: $\det(J) < 0$.
Left: case 1. ($\det(\Phi) > 0$). Middle: case 2.(a) ($\det(\Phi) < 0$ , $\phi_{11}, \phi_{22}$ and $\phi_{11} + \phi_{22} - 2\phi_{12}$ all have the same sign). Right: Case 2.(b) ($\det(\Phi) < 0$ , $\phi_{11}, \phi_{22}$ and $\phi_{11} + \phi_{22} - 2\phi_{12}$ do not all have the same sign).

Fig. 4: Illustration of Proof of Lemma 4 (Hopf bifurcations for equilibria with mutation, $\alpha \neq 0$, $\kappa_1 = \kappa_2$)
Conic sections: zeros of $\mathrm{tr}(J)$ as in eq. (6.18). Bold straight lines: zeros of $\det(J)$ as in eq. (6.17). Thin straight lines: $B_1B_2$–edge of $S_2$.
For further explanations, see Fig. 3.

Fig. 5: Illustration of Proof of Theorem 1 (Hopf bifurcations for equilibria with mutation, $\alpha \neq 0$, $\tilde{c}_2 \neq 0$)
Conic sections: zeros of $\mathrm{tr}(J)$ as in eq. (6.27). Bold straight lines: zeros of $\det(J)$ as in eq. (6.26). Thin straight lines: $B_1B_2$–edge of $S_2$.
For further explanations, see Fig. 3.

Fig. 6: Fitness landscape and phase portraits of the diploid three-class model (6.20) for various values of $\mu$. Sequence lengths: $\kappa_1 = 30$, $\kappa_2 = 10$. Fitness parameters: $\phi_{11} = 5.705$, $\phi_{12} = 4.572$, $\phi_{22} = 4.403$, $r_1 = 2.327$, $r_2 = 0.579$, or, equivalently, $w_{11} = 10.363$, $w_{12} = 7.482$, $w_{13} = 2.331$, $w_{22} = 5.565$, $w_{23} = 0.583$, $w_{33} = 0$. Upper left: contour plot of mean fitness (fitness increases with darkness of shading). Upper right: $\mu = 0$. From middle left to lower right: $\mu = 0.08,\ 0.1,\ 0.12,\ 0.15$. Horizontal axes: $y_1$; vertical axes: $y_2$, $0 \leq y_1, y_2 \leq 1$.

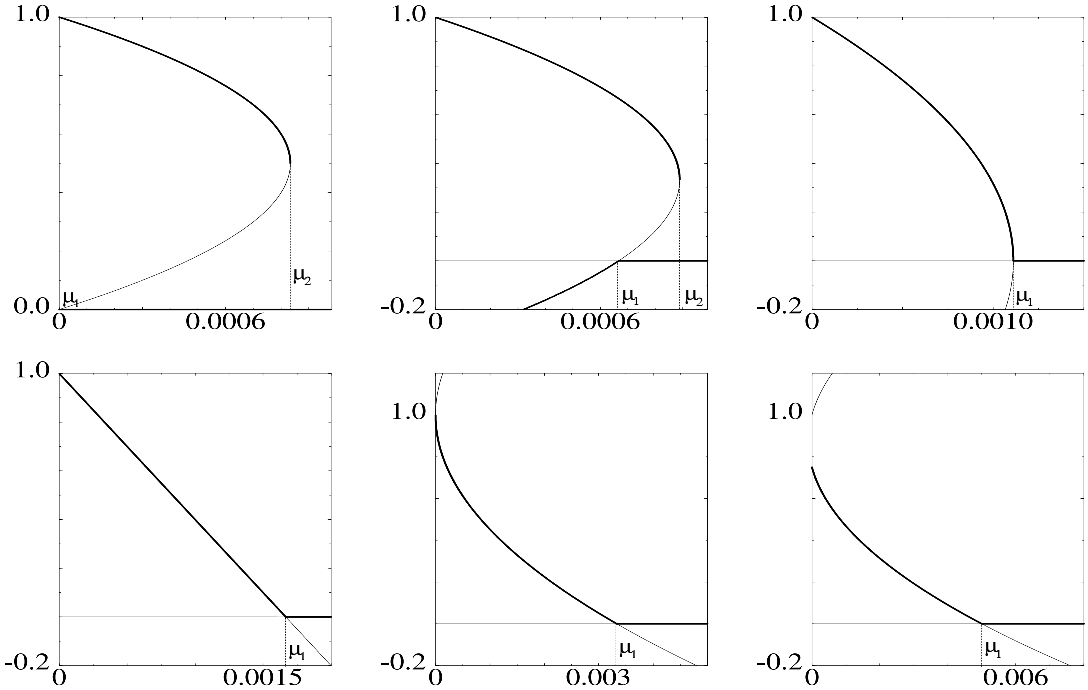

1.0
0.0
0
0.0006
μ1
μ2
1.0
-0.2
0
0.0006
μ1
μ2
1.0
-0.2
0
0.0010
μ1
1.0
-0.2
0
0.0015
μ1
1.0
-0.2
0
0.003
μ1
1.0
-0.2
0
0.006
μ1

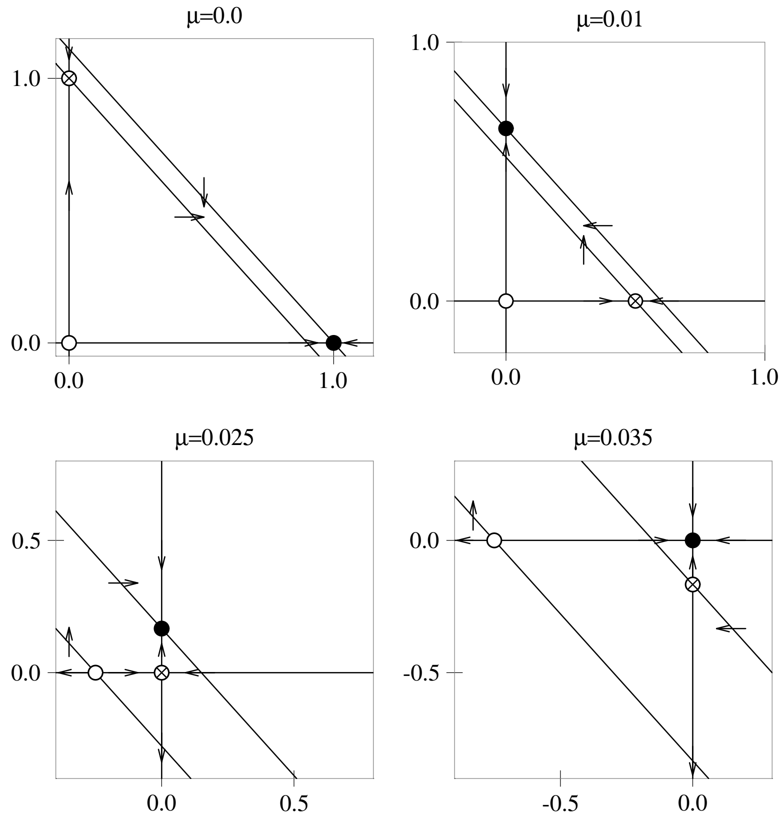

μ=0.0
1.0
0.0
0.0
1.0
μ=0.01
1.0
0.0
0.0
1.0
μ=0.025
0.5
0.0
0.0
0.5
μ=0.035
0.0
-0.5
-0.5
0.0

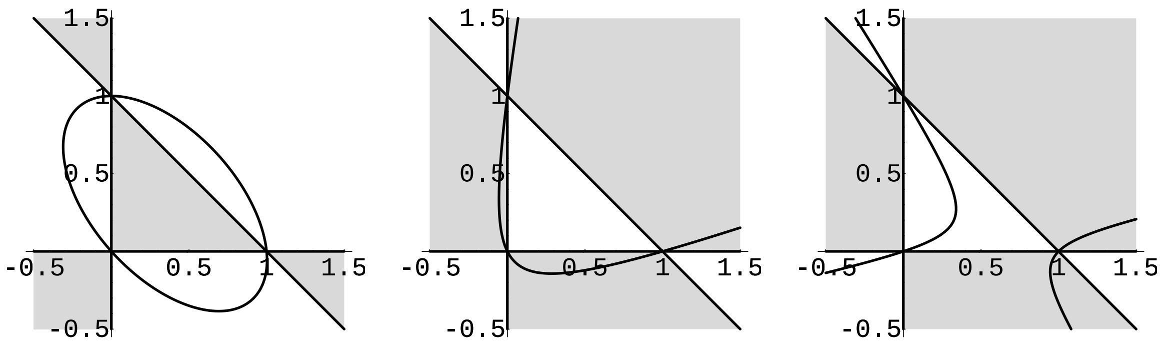

1.5
1
0.5
-0.5
0.5
1
1.5
-0.5

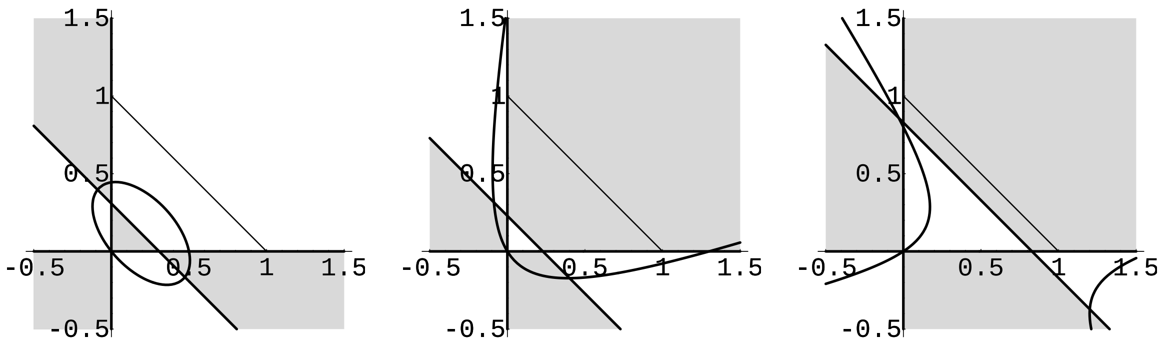

1.5
1
0.5
-0.5
0.5
1
1.5
-0.5
1.5
1
0.5
-0.5
0.5
1
1.5
-0.5
1.5
1
0.5
-0.5
0.5
1
1.5
-0.5

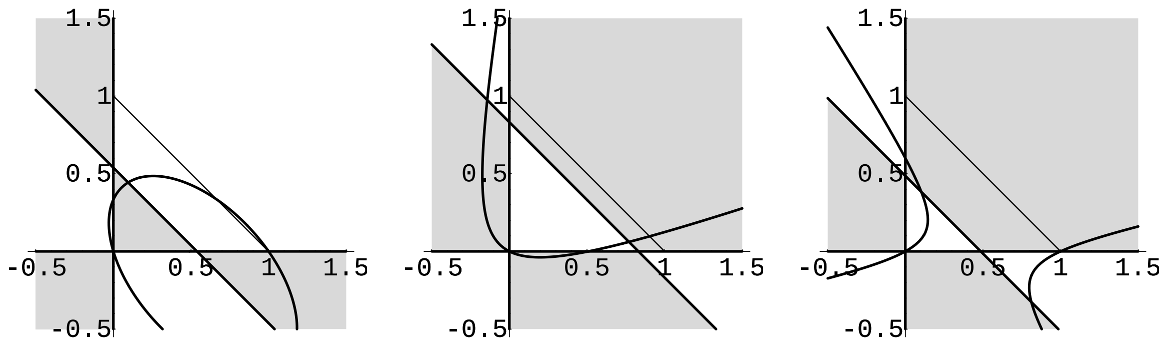
1.5
1
0.5
-0.5
0.5
1
1.5
-0.5
1.5
1
0.5
-0.5
0.5
1
1.5
-0.5
1.5
1
0.5
-0.5
0.5
1
1.5
-0.5